

HYDROTHERMAL SYNTHESIS OF BEIDELLITES: CHARACTERIZATION AND STUDY OF THE *CIS*- AND *TRANS*-VACANT CHARACTER

SÉBASTIEN LANTENOIS^{1,2,*}, FABRICE MULLER¹, JEAN-MICHEL BÉNY¹, JAMEL MAHIAOUI²,
AND RÉMI CHAMPALLIER¹

¹ Institut des Sciences de la Terre d'Orléans (ISTO), CNRS – Université d'Orléans, 1A rue de la Férellerie, 45071 Orléans Cedex 2, France

² Institut Charles Gerhardt, AIME (Agrégats, Interfaces et Matériaux pour l'Energie) CNRS – Université Montpellier 2, UMR 5253, CC 015, Place Eugène Bataillon, 34095 Montpellier Cedex 5, France

Abstract—Low-charge beidellites were synthesized by a hydrothermal treatment applied to an amorphous gel phase in basic solution. The hydrothermal conditions for the syntheses were chosen from the stability field of beidellite previously investigated in the literature. The synthetic samples were characterized chemically and structurally using X-ray diffraction, infrared spectroscopy, cation exchange capacity measurement, and chemical and thermal analyses. We compared the synthetic sample with a natural beidellite sample (Sbld) from Idaho, USA, looking at chemical composition and particle size. The main difference is the octahedral site occupancy (*cis*- or *trans*-vacant layer structure). The natural Sbld sample has *trans*-vacant layers and the synthetic sample has a preferentially *cis*-vacant character. This character can be modulated, using specific synthesis conditions. The *cis*- or *trans*-vacant layer structure of various synthetic beidellites was investigated at low temperature (<350°C) and pressure (<25 MPa). Depending on the pressure and/or synthesis temperature, the proportion of *cis*-vacant layers ranges from 20 to 100% and increases with the layer-charge deficit.

Key Words—Beidellite, Chemical Analyses, *Cis*-vacant Layer, FTIR Spectroscopy, Hydrothermal Syntheses, Smectite, TGA, *Trans*-vacant Layer, XRD.

INTRODUCTION

Swelling clays are among the most common phyllosilicates found in soils and sediments. Their large specific surface area, large cation exchange capacities, and hydration properties cause these clays to be industrially attractive. They have numerous applications (e.g. in nanocomposite science, ceramics, waste confinement, and soil decontamination). The swelling clay group includes natural smectites, depending on the chemical composition and on the partition of the layer-charge deficit between tetrahedral and octahedral sheets. Montmorillonite is an alumino-phyllosilicate for which Al in octahedral sheets is substituted by Mg (Caillere *et al.*, 1982). Beidellite and nontronite are phyllosilicates containing principally Al or ferric Fe in the octahedral sheets, respectively. Their charge deficit is mainly located in the tetrahedral sheets by substitution of Al for Si. Such differences in mineralogical composition, charge deficit, and structural and microstructural characteristics lead to important variations in their properties, e.g. the location of the layer-charge deficit is one of the main parameters influencing the transformation of smectites to illite during diagenesis. In order to associate the differences in behavior of smectites with specific

chemical or structural properties, the study of a set of samples with only one parameter modified between two of them is necessary. The precise management of chemical composition and substitutions is, however, very difficult with natural samples. The only way to solve this problem is to use synthetic samples.

Few studies in the last 40 y have focused on the experimental conditions of synthesis of smectites, in order to determine the stability fields of these phases. All of these studies were summarized in a critical review by Klopogge *et al.* (1999). Using these stability fields as guidelines, it is possible to synthesize beidellites (Klopogge *et al.*, 1990, 1993; Grauby *et al.*, 1993), saponites (Suquet *et al.*, 1977, 1982; Grauby *et al.*, 1993), hectorites (Torii *et al.*, 1983; Torii, 1985; Torii and Iwasaki, 1986, 1987), nontronites (Decarreau *et al.*, 1987), and montmorillonites (Nakazawa *et al.*, 1991; Yamada *et al.*, 1991, 1994; Lantenois *et al.*, 2007a). These last studies highlighted the difficulties involved in the synthesis of high-purity smectite with the desired chemical composition. Saponites with various layer-charge deficits were synthesized and characterized by Suquet *et al.* (1977). However, synthesis of montmorillonites with variable layer-charge deficits is difficult (Lantenois *et al.*, 2007a).

The aim of this study was to synthesize beidellite samples with crystallographic structures close to those of natural samples. In the first part of this work, a bibliographic study was used to determine the more suitable hydrothermal conditions to synthesize Na-

* E-mail address of corresponding author:
sebastien.lantenois@univ-montp2.fr
DOI: 10.1346/CCMN.2008.0560104

beidellites. The second part was a comparative study of a synthetic sample and a natural sample, showing that the main difference between them is the proportion of *cis*-vacant layers, *i.e.* $C/(C+T)$ (number of *cis*-vacant layers/total number of layers). The third part was devoted to the synthesis and study of a set of beidellites with increasing layer-charge deficit ($0.30 < x < 0.6$). Different $C/(C+T)$ ratios were investigated.

The samples were characterized by electron microprobe (EMP), powder X-ray diffraction (XRD), fast Fourier transform infrared spectroscopy (FTIR), thermogravimetric analysis (TGA), nitrogen adsorption, and cation exchange capacity (CEC) measurements.

EXPERIMENTAL PROCEDURES

Starting materials

The synthetic clay samples were crystallized from gels under hydrothermal conditions. The chemical composition of the gel phases was chosen to correspond to the ideal chemical composition of the required smectite phase. Three gels were synthesized corresponding to three chemical compositions of beidellite phases $[\text{Na}_x(\text{Al})_2(\text{Si}_{4-x}\text{Al}_x)\text{O}_{10}(\text{OH})_2]$ with $x = 0.33, 0.5, \text{ or } 0.6$.

Gels were prepared following the method adapted from Hamilton and Henderson (1968) using tetraethylorthosilicate (TEOS) as the silicon source, $\text{Al}(\text{NO}_3)_3 \cdot 9\text{H}_2\text{O}$, HNO_3 , Na_2CO_3 , NH_4OH , and ethanol as reagents with a 99% minimum grade purity. After dissolution of Al-nitrates and Na_2CO_3 in nitric acid, TEOS and ethanol were added. A precipitate was obtained by neutralizing the resulting solution at $\text{pH} \approx 6$ with the addition of NH_4OH . This precipitate was dried at 80°C for 24 h, ground in an agate mortar, and then heated to 400°C in order to obtain an Al, Si, and Na oxide gel, without nitrates or carbonates.

The chemical compositions of the three gel phases were measured by inductively coupled plasma-atomic emission spectroscopy (ICP-AES) and are reported in Table 1.

Table 1. Chemical composition (wt.% oxide normalized to 100%) of starting gel phases measured by ICP-AES. x is the interlayer Na cation content per half unit cell.

Sample	GB1	GB2	GB3
x	0.33	0.50	0.60
SiO_2	59.0	57.1	53.8
Al_2O_3	38.4	39.8	42.6
Na_2O	2.4	3.1	3.6

The natural beidellite sample (SbId) was obtained from The Clay Minerals Society Source Clays Repository. The raw sample was ground in an agate mortar, purified by sodium exchange and elimination of $>2 \mu\text{m}$ material.

Hydrothermal syntheses

Two types of hydrothermal experiments were used, depending on the required pressure domain. At a fixed pressure of 25 MPa, the samples were synthesized in an internally heated pressure vessel. A gel phase and a NaOH (0.2 N) solution (weight ratio of $\frac{1}{2}$) were loaded in a gold tube. This tube was then sealed and heated to 350°C under controlled argon pressure.

At pressures between 2.5 MPa and 11.5 MPa, samples were synthesized in a cold-sealed pressure vessel. The gel phase and the NaOH (0.2 N) solution (weight ratio of $\frac{1}{2}$) were placed in a gold capsule and then placed in a Prolabo[®] metallic vessel. In this case, the pressure was imposed by the water pressure at equilibrium, which was calculated for the synthesis temperatures.

Experimental runs were performed with different starting gel phases at various pressure and temperature conditions (reported in Table 2). After cooling of the vessels, the solid products were extracted from the reaction tubes, dried at 80°C overnight and ground before structural and chemical characterization.

Table 2. Experimental conditions and reaction products of the experiments.

Sample name	Starting gel phase	Starting solution	Duration (days)	T ($^\circ\text{C}$)	P (MPa)	Product*
SB1-350	GB1	NaOH (0.2 M)	15	350	25 ^a	Beid
SB1-325	GB1	NaOH (0.2 M)	15	325	11.5 ^b	Beid
SB1-280	GB1	NaOH (0.2 M)	15	280	7.5 ^b	Beid, Kaol
SB1-250	GB1	NaOH (0.2 M)	15	250	3 ^b	—
SB2-350	GB2	NaOH (0.2 M)	15	350	25 ^a	Beid, Para
SB2-325	GB2	NaOH (0.2 M)	15	325	11.5 ^b	Beid
SB2-280	GB2	NaOH (0.2 M)	15	280	7.5 ^b	Beid
SB3-350	GB3	NaOH (0.2 M)	15	350	25 ^a	Beid, Para
SB3-325	GB3	NaOH (0.2 M)	15	325	11.5 ^b	Beid
SB3-280	GB3	NaOH (0.2 M)	15	280	7.5 ^b	Beid

* Crystalline phases identified by XRD.

Beid: beidellite; Para: paragonite; Kaol: kaolinite.

^a pressure imposed on the system

^b estimated pressure

Characterization

The chemical compositions of the starting gel phases were checked by inductively coupled plasma-atomic emission spectroscopy (ICP-AES) analysis using a JOBIN-YVON ULTIMA spectrometer. 100 mg of gels were dissolved by acid attack after an alkaline fusion and the Si, Al, and Na concentrations were measured.

The chemical compositions of the synthesized products were checked using EMPA (CAMECA SX50 electron microprobe operating at 15 kV accelerating voltage). The samples analyzed had been washed in ethanol and then dialyzed in de-ionized water for 1 week to remove excess Na initially present in solution. After dialysis, the $<2\ \mu\text{m}$ size fraction of the samples, which corresponds mainly to the clay fraction, was extracted, dried, and finely ground in an agate mortar. To obtain optimal EMPA results, the physical surface of the samples must be flat. Consequently, the sample powders were pressed into an evacuable die in order to prepare a pellet. This pellet was fixed on a glass slide and then sputter-coated with carbon before analysis.

Powder XRD transmission patterns were recorded using $\text{CoK}\alpha$ radiation (35 mA, 35 kV). The use of an INEL CPS 120 curved, position-sensitive detector allowed instantaneous recording of the diffracted intensity over a $4\text{--}120^\circ 2\theta$ range with a $0.03^\circ 2\theta$ step size. The non-linearity of the detector response was corrected (Roux and Volfinger, 1996). A 0.5 mm diameter Lindemann glass tube was used to hold the sample powder. In order to characterize the synthetic beidellite by its swelling behavior, the layer swelling due to ethylene glycol (EG) intercalation and collapse induced by the loss of interlayer water was realized as follows. The smectite samples were placed in XRD glass tubes. These tubes were heated overnight at 110°C and then placed in a desiccator under EG atmosphere for 24 h before they were sealed and analyzed. For the collapse experiments, samples were heated overnight at 250°C in the XRD glass tubes. These tubes were then sealed and placed in the diffractometer.

Infrared (FTIR) spectra were recorded using a Nicolet Magna-IR 760 Fourier transform spectrometer equipped with a Nicolet Nic-Plan microscope and Nicolet MCT-A detector. The clay powder was then spread over the NaCl window of the microscope stage, using the microscope's $15\times$ Cassegrainian objective lenses, a $100\ \mu\text{m}$ diameter spot of the clay powder was analyzed. Spectra were acquired with 200 scans at a resolution of $2\ \text{cm}^{-1}$ over the range of 650 to $4000\ \text{cm}^{-1}$. To minimize the contributions to the spectra of atmospheric H_2O and CO_2 , and water adsorbed to the clay, the instrument was purged with dry and CO_2 -free air.

The cation exchange capacity (CEC) was measured using the copper complex method of Gaboriau (1991), for which 600 mg of the sample were suspended for 12 h in 25 mL of a 0.02 N ethylene diamine copper complex ($\text{Cu}(\text{EDA})_2\text{Cl}_2$) solution. After centrifugation, the Cu

concentration in solution was measured using a GBC Scientific Model 905 atomic absorption spectrophotometer.

The adsorption/desorption isotherms of nitrogen at 77 K were measured using a Micromeritics ASAP 2010 instrument. Smectite samples (80 mg) were outgassed overnight at 200°C . The specific surface areas were calculated using adsorption data in the relative pressure range from 0.10 to 0.28 included in the validity of the BET equation (Gregg and Sing, 1982). The BET specific surface area was calculated using a cross-sectional area of $0.162\ \text{nm}^2$ per nitrogen molecule, following I.U.P.A.C. recommendations.

A Raman spectrum was obtained using a Dilor XY 800 confocal micro-Raman spectrometer equipped with a Wright charge-coupled device detector (CCD). The excitation source was the $514\ \text{nm}$ green line of a Coherent Innova Model 90-5 Ar^+ laser. The beam was focused onto the sample powder placed on a glass slide using a $100\times$ objective. Measurements were carried out using laser power of 100 mW and an integration time of 300 s.

The thermogravimetric analyses (TGA) were recorded using a NETZSCH STA409PC microanalyzer, with heating rate of $10^\circ\text{C}/\text{min}$. A 60 mg sample was used for each measurement. The derivative of the TG curve (DTG) gives the weight loss, which was assigned to the loss of adsorbed and interlayer water (between 20 and 200°C), *i.e.* to water evolved from hydroxyl groups associated with the *trans*-vacant smectite structure near 500°C and to the *cis*-vacant smectite structure near 700°C (see Discussion). The quantification of the proportion of *cis*- and *trans*-vacant smectite layers was performed using DTG curves and an etalon curve obtained using different mixtures of natural *trans*- and *cis*-vacant samples. Mixtures of the $<2\ \mu\text{m}$ fraction of Na-exchanged SbId beidellite (*trans*-vacant smectite) and SWy-2 montmorillonite (*cis*-vacant smectite) were obtained from different mass ratios. The area under the curve of dehydroxylation peaks between 375 and 575°C for *trans*-vacant structures and between 575 and 775°C for *cis*-vacant structures (as shown in Figure 1) were measured after subtraction of a linear baseline between

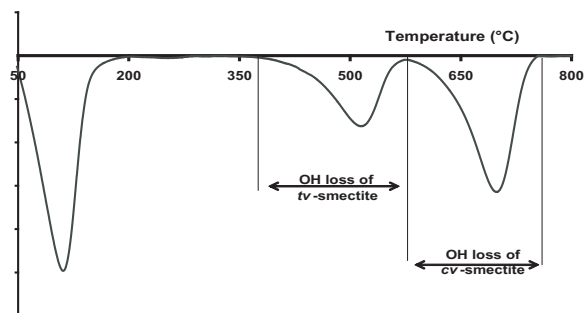


Figure 1. DTG curve of a mixture of SbId (40 wt.%) *trans*-vacant smectite and SWy-2 (60 wt.%) *cis*-vacant smectite.

300 and 800°C. The relative proportion of *cis*- and *trans*-vacant layers was correlated to the initial weight of samples introduced in the mixtures.

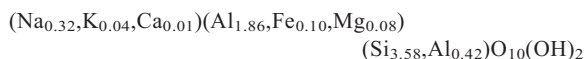
RESULTS AND DISCUSSION

Choice of experimental conditions

A few studies have focused on the experimental conditions of beidellite synthesis in order to map the stability fields of this phase (Roy and Sand, 1956; Grandquist and Pollack, 1967; Grandquist *et al.*, 1972; De Kimpe, 1976; Eberl, 1978; Yamada *et al.*, 1991; Klopogge *et al.*, 1990, 1993). The pressure-temperature diagram which summarizes almost all the experimental data was given by Klopogge *et al.* (1999). The stability field range deduced from this study is 270–470°C and 0–300 MPa. Unfortunately, in these hydrothermal conditions, other phases can be formed. Rectorite, quartz, and cristobalite are obtained at high pressures and high temperatures in this range. Kaolinite is synthesized between 200 and 300°C and paragonite is obtained from 400°C (Klopogge *et al.*, 1999; Klopogge, 2006). In order to obtain beidellite only, it is necessary to restrict the hydrothermal conditions to 300–400°C and 0–50 MPa. Moreover, in order to obtain the maximum amount of synthetic product, it is necessary to set the duration of the synthesis process to >10 days (Klopogge, 2006). We set our experimental conditions at 350°C and 25 MPa for 15 days, and these conditions worked well. The purpose here was to compare a synthetic beidellite and the natural SbId beidellite. Therefore, the tetrahedral deficit of charge per half unit cell (*x*) was fixed at 0.3 for the synthetic beidellite used for the comparison. In addition to this synthetic beidellite, other beidellite samples have been synthesized at lower temperature and pressure conditions. The objective was to modify the crystallographic structure of synthetic beidellites. All experimental conditions are reported in Table 2.

Comparison of synthetic and natural beidellite

The sample SB1-350 was characterized and compared to the natural beidellite, SbId. In the two samples, only a smectite phase was clearly identified on the XRD pattern (Figure 2) with the characteristic reflections (001; 02,11; 20,13) described in the literature (MacEwan and Brown, 1961). These smectite phases can be collapsed after heating or expanded after EG intercalation (Figure 2, heating and EG). The similarity between the patterns of the synthetic and natural samples confirms that the synthetic product is indeed a beidellite. The chemical formulae were determined by microprobe analyses. The structural formula of the natural SbId sample is as follows:



The chemical formula of the SB1-350 synthetic sample is close to the initial set formula (Table 3). Except for the lack of structural Fe and Mg in the octahedral sheet and of K and Ca in the interlayer space, the chemical composition of the synthetic beidellite is very close to that of the natural sample.

Nevertheless, some differences between the two samples are observed. Firstly, the associated phases identified with these two samples are an amorphous residual phase in synthetic SB1-350 (according to Klopogge *et al.*, 1993) and mineral phases such as anatase and kaolinite (Lantenois, 2003) in the SBId sample. The presence of anatase is observed in XRD patterns (Figure 2, labeled with a star) and is confirmed by the Raman spectrum (Figure 3) in which characteristic vibration bands at 144, 395, 516, and 639 cm^{-1} are observed. Secondly, the hydration characteristics of the two samples (Table 4) showed some differences. The synthetic beidellite can be more hydrated (10.5 g of water/100 g of sample in comparison with 9.3 g/100 g for SbId; TGA data, Table 4). This might be due to the smaller size of the synthetic smectite particles. Indeed, if the mean number of stacked layers (determined by XRD, Table 4) is nearly the same (7.5 and 8 layers), in accordance with the classical results obtained by Besson (1980) for natural

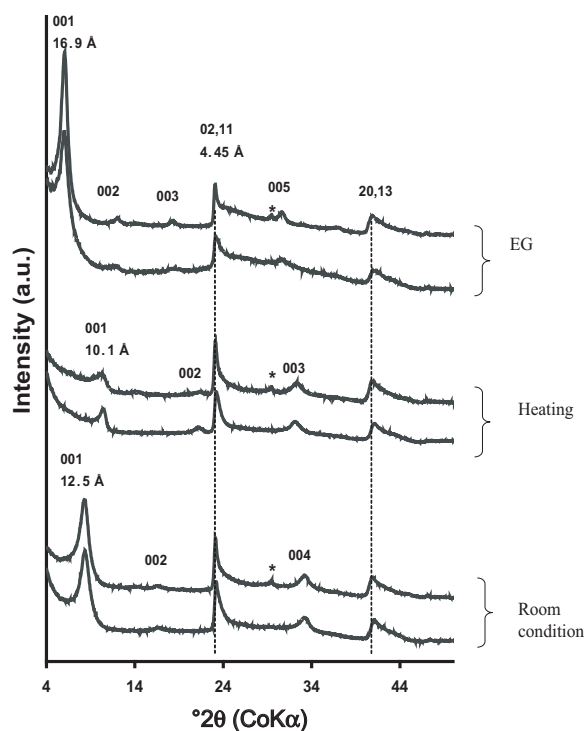


Figure 2. XRD patterns of synthetic SB1-350 and natural SbId beidellite samples (lower and upper patterns, respectively) in room conditions, after heating at 500°C and after ethylene glycol saturation. The dashed lines indicate smectite band positions. 001 reflections are noted above the corresponding peak. The * corresponds to a reflection of anatase.

Table 3. Chemical composition of the synthetic smectites obtained by chemical and microprobe analyses.

	GB1*	GB2*	GB3*	SB1-350	SB1-325	SB1-280	SB1-250	SB2-350	SB3-350	SB2-325	SB3-325
Tetrahedral											
Si	3.66	3.50	3.32	3.60	3.61	3.62	—	3.52	3.31	3.48	3.32
Al	0.34	0.50	0.68	0.40	0.39	0.38	—	0.52	0.69	0.48	0.68
Octahedral											
Al	2.00	2.00	2.00	2.00	2.00	2.00	—	2.00	2.00	2.00	2.00
Interlayer											
Na	0.31	0.46	0.58	0.38	0.40	0.33	—	0.50	0.68	0.46	0.67
CEC**				98	94	78	25	90	87	108	129

* theoretical formulae calculated using chemical analyses in Table 1. The structural formulae were calculated per $O_{10}(OH)_2$.

**CEC: cation exchange capacity (meq/100 g of calcined clay).

smectite samples, then the surface area determined using nitrogen adsorption and BET model calculation (Cases *et al.*, 1992) is estimated to be 20 m^2/g for the natural beidellite and 95 m^2/g for the synthetic one. This difference can be attributed to the particle size and can then explain the different hydration properties found here.

The *cis*- and *trans*-vacant layer character

The most important difference between the two samples is shown by thermogravimetric analyses (Figure 4). On the DTG curves, the dehydroxylation reaches a maximum rate at 520°C for the natural SbId sample and at ~700°C for the synthetic one. This difference in dehydroxylation temperature can be explained from a structural point of view (Drits *et al.*, 1995; Muller *et al.*, 2000). The layers of dioctahedral 2:1 phyllosilicates can differ by their distribution of octahedral cations over the *trans*- and *cis*-vacant sites (Figures 5a and 5b, respectively). In dioctahedral phyllosilicates, the octahedral sheet is composed of two cations and a vacancy around the OH group. If the two cations are placed in *cis*-sites the structure is identified as a *trans*-vacant structure (Figure 5a). On the contrary, if one cation is placed in the *trans*-site and the second in one of the two *cis*-sites, the structure is identified as a *cis*-vacant structure (Figure 5b).

Basically, the thermal energy needed for a proton to jump to the nearest OH group to form a water molecule

depends on the distance between the nearest OH groups (Drits *et al.*, 1995). Therefore a *cis*-vacant structure should require greater dehydroxylation energy than a *trans*-vacant structure because of the greater OH–OH distance (Muller *et al.*, 2000) and the additional thermal energy required to provide migration of cations from *trans*-sites to the initial nearest *cis*-vacant sites (Drits, 2003). This explanation is confirmed in the literature by the observation of two dehydroxylation temperature ranges. The *trans*-vacant smectites dehydroxylate between 500 and 675°C and *cis*-vacant ones dehydroxylate between 675 and 800°C (Trauth and Lucas, 1967; Mackenzie, 1970; Tshipursky *et al.*, 1985; Drits *et al.*, 1995; Muller *et al.*, 2000). The synthetic beidellite has *cis*-vacant layers unlike the natural beidellite which is a *trans*-vacant smectite.

Quantification of the ratio of *cis*- and *trans*-vacant layers

Thermogravimetric analysis can be used in order to quantify the number of water molecules eliminated as a function of temperature. However, this technique is

Table 4. Surface and adsorption characteristics of natural SbId and synthetic SB1-350.

	SbId	SB1-350
CEC (meq/100 g)	96	98
Amount of adsorbed water (g/100 g) ¹	9.3	10.5
<i>T</i> (°C) of water evaporation ²	111	102
BET surface area (m^2/g)	20	95
\bar{M} (stacking layers) ³	8	7.5

¹ Calculated in g per 100g of calcined clay, using TGA measurements (Figure 5)

² Obtained by TGA measurements (Figure 5)

³ Mean number of stacking layers calculated using the Scherrer formula $\bar{M} = K \frac{1}{d_{001}} \frac{\lambda}{\beta \cos \theta}$ (Moore and Reynolds, 1997) with *K*, a constant, ≈ 1 , λ the wavelength in Å, d_{001} in Å, and β the full width at half maximum of the 001 reflection in radian. Calculated at room conditions (38% relative humidity) using the XRD trace in Figure 1.

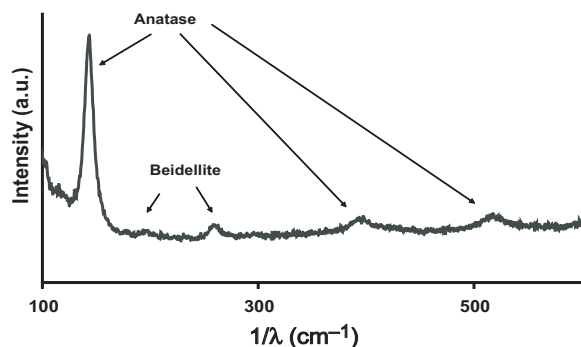


Figure 3. Raman spectrum of a natural SbId sample.

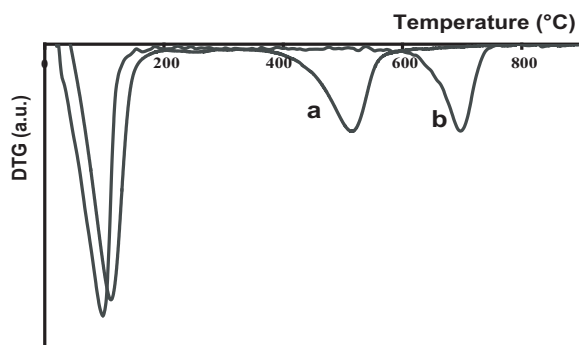


Figure 4. DTG curves of natural SbId (a) and synthetic SB1-350 (b) beidellites.

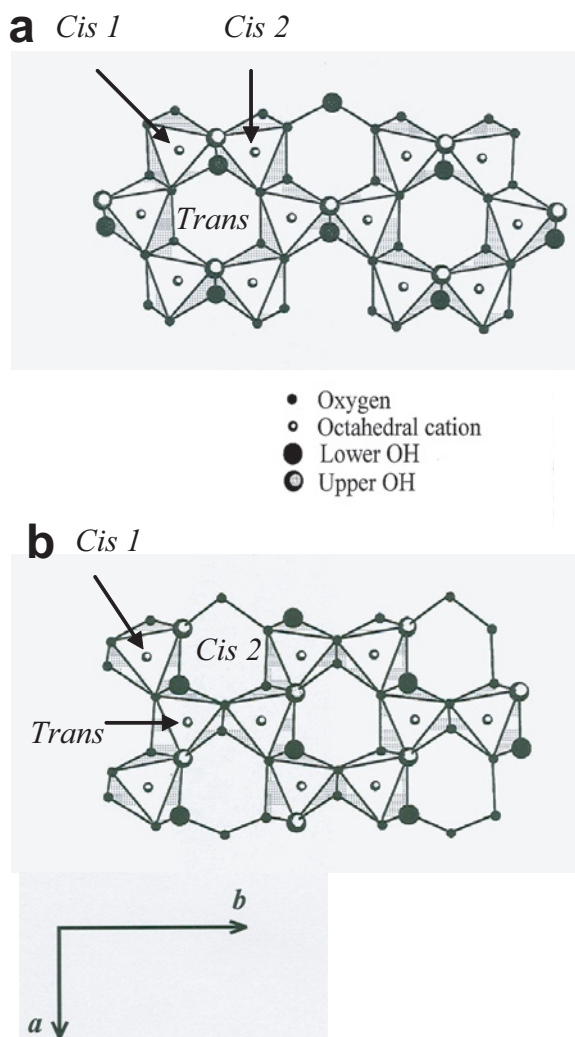


Figure 5. Schematic representation of an octahedral sheet in the case of *trans*-vacant layers (a) and *cis*-vacant layers (b).

commonly coupled with a water detection system in order to discriminate water molecules from other molecules which can also be present in natural samples. Either TGA-MS (Drits and McCarty, 2007) or TGA coupled with evolved water analysis (EWA) using an IR detector (Drits *et al.*, 1998) can be used to quantify the loss of water molecules.

In the case of our synthetic samples, the smectite phase is only associated with a small amount of residual amorphous phase. This phase can have a small number of OH groups on the surface, which are eliminated during thermal treatment. The temperature range corresponding to this water loss is 200–900°C (Lantenois *et al.*, 2007a). This identification assumes that only structural OH groups of smectite are eliminated in the range 375–775°C, an assumption which is valid only for very pure samples. Figure 6 shows that the proportion of *trans*-vacant layers is equal to the proportion of SbId sample in the mixture and proves the validity of the method with a $\pm 5\%$ estimated error. According to this analysis, the amount of *cis*- and *trans*-vacant layers synthesized can be calculated.

Evolution of the cis- and trans-vacant layer character

Natural beidellites have been studied extensively and generally have *trans*-vacant structures (Tsipursky and Drits, 1984). For example, the most studied natural samples: SbId (this study, Figure 3), Black Jack Mine (Greene-Kelly, 1957), and Wyoming (Trauth and Lucas, 1967) beidellites showed a maximum dehydroxylation peak near 550°C. Klopogge *et al.* (1990) showed that at high pressure and high temperature conditions (350°C and 10 MPa), synthetic beidellites have a dehydroxylation temperature near 700°C, which is characteristic of *cis*-vacant structure. It is known that the $C/(C+T)$ ratio can be modified after heating and hydrothermal treatment (Muller *et al.*, 2000, 2002). However, with changing synthesis conditions it is also possible to obtain synthetic clays with different $C/(C+T)$ ratios (Lantenois *et al.*, 2007b).

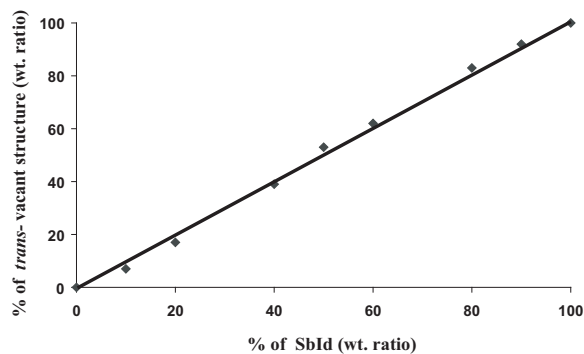


Figure 6. Comparison between various proportions of beidellite (*trans*-vacant structure) introduced into a mixture with SWy-2 montmorillonite (*cis*-vacant structure), and the amounts of *trans*-vacant structure determined using DTG measurements.

The hydrothermal conditions required to synthesize samples SB1-325, SB1-280, and SB1-250 are reported in Table 2. The corresponding XRD patterns are displayed in Figure 7. The SB1-325 and SB1-280 patterns (Figure 7b,c) are typical of a pure beidellite smectite phase. The SB1-250 (Figure 7d) pattern only shows the presence of an amorphous phase, corresponding to the initial gel phase. The chemical formulae of the synthetic beidellite samples (SB1-325 and SB1-280) were calculated using the $<2 \mu\text{m}$ size clay fraction and the CEC values were measured (Table 3). The results show that the structural formulae of these two synthetic beidellites are similar and close to the formula for sample SB1-350. Only a decrease in the CEC is observed for SB1-280, which indicates a smaller amount of synthesized beidellite. The *cis/trans*-vacant character of these samples was investigated by TGA measurements (Figure 8). The temperature corresponding to the maximum degree of dehydroxylation is near 680°C for sample SB1-350. This result is in accord with those of Klopogge *et al.* (1990). Contrary to this result, two

maxima were observed for the SB1-325 and SB1-280 samples: the first near 460°C and the second near 680°C . These two samples contain *cis*- and *trans*-vacant layers. The $C/(C+T)$ ratio is estimated at 100%, 70% and 20% for samples SB1-350, SB1-325, and SB1-280, respectively. This ratio was modified with different synthesis conditions. *Trans*-vacant structures appear at lower pressure/temperature conditions.

Influence of layer-charge deficit on cis/trans-vacant ratio

SBld natural beidellites have a charge deficit close to 0.33 per half unit cell, corresponding to the theoretical layer-charge deficit of a beidellite (MacEwan and Brown, 1961). Nevertheless, heterogeneities in the chemical compositions have been observed in natural beidellites and the layer-charge deficit of these beidellites ranged from 0.33 and 0.6 per half unit cell. For example, the beidellite from Black Jack Mine has a charge deficit close to 0.54 per half unit cell (Weir and Greene-Kelly, 1962). Synthetic beidellites with various layer-charge deficits can also be obtained using different chemical compositions of the initial gel phases (Klopogge *et al.*, 1993).

We have synthesized two beidellite sets using an initial gel phase containing less Si and more Al and Na (GB2 and GB3, Table 1). The same pressure and/or temperature conditions as those for the SB1 beidellites were used (Table 2).

The synthetic samples SB2-350 and SB3-350 were synthesized at 350°C and 25 MPa. The XRD patterns (Figure 7e,h) indicated the presence of synthetic beidellite phases associated with paragonite, which is not a swelling clay phase and which contains more Na than beidellite. The presence of the paragonite phase, $(\text{Na}(\text{Si}_3\text{Al})\text{Al}_2\text{O}_{10}(\text{OH})_2)$, indicates that in this mixture, the synthetic beidellite phase does not have a larger layer-charge deficit than the SB1-350 beidellite. However, beidellites with greater layer-charge deficit can be synthesized at low pressure and temperature; *e.g.* at 325°C and 11.5 MPa, the XRD patterns of the SB2-325 and SB3-325 samples showed that only beidellites are synthesized (Figure 7f,i). The chemical compositions of

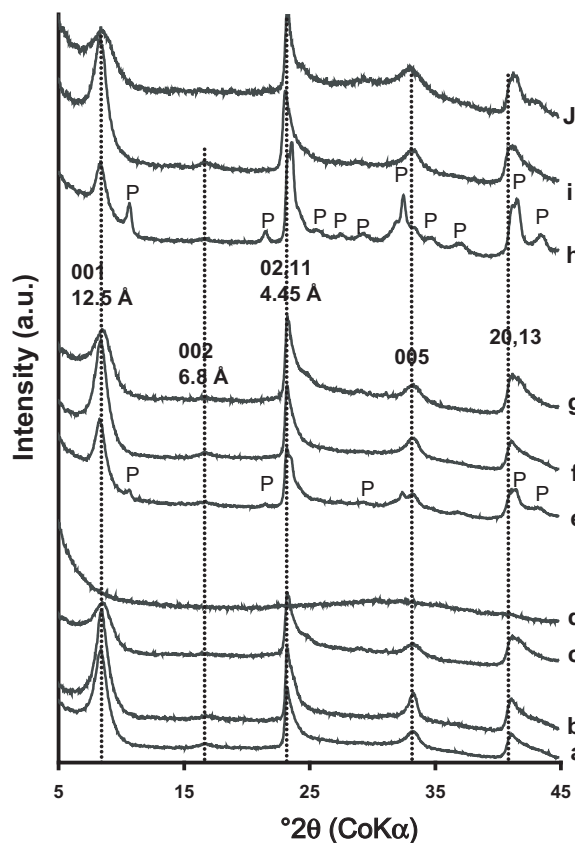


Figure 7. XRD patterns of synthetic beidellite samples: (a) SB1-350; (b) SB1-325; (c) SB1-280; (d) SB1-250; (e) SB2-350; (f) SB2-325; (g) SB2-280; (h) SB3-250; (i) SB3-225; and (j) SB3-280. Dotted lines correspond to beidellite 001 reflections and to 02,11 and 20,13 bands. The characteristic bands of paragonite (P) are identified in the SB2-350 and SB3-350 samples.

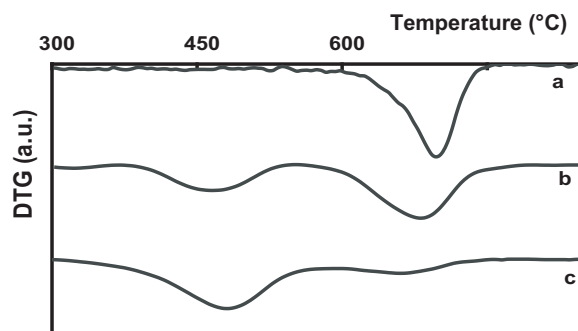


Figure 8. DTG curves of synthetic beidellites SB1-350 (a), SB1-325 (b) and SB1-280 (c).

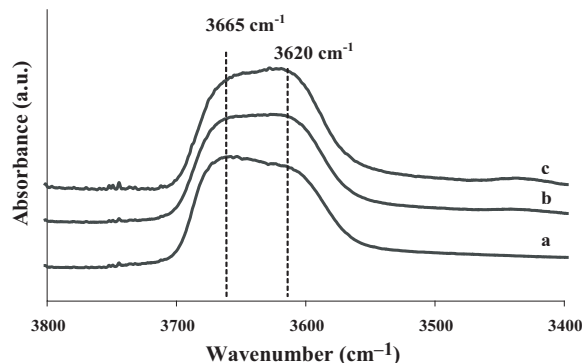


Figure 9. IR spectra in the OH-stretching zone of synthetic beidellite samples SB1-325 (a), SB2-325 (b), and SB3-325 (c).

these beidellites have been calculated (Table 3). Data indicate that the synthetic beidellite phases have more layer-charge deficits compared to sample SB1-325. These results are confirmed by the increase in CEC from SB1-325 to SB3-225 (Table 3). The increase in layer-charge deficit can also be shown by an IR study. In the stretching zone (between 3500 and 3700 cm^{-1}), the Al-Al-OH vibrations of smectites can be observed at 3620–3680 cm^{-1} (Gates, 2004). Besson and Drits (1997a,b) identified two types of bands: “pyrophyllite type” bands corresponding to Al-Al-OH vibrations without interlayer cations, and “mica type” bands corresponding to Al-Al-OH vibrations associated with a tetrahedral substitution of Si by Al and the presence of an interlayer cation to balance the charge deficit. Zviagina *et al.* (2004) fixed these bands in smectites near 3670 cm^{-1} and 3640 cm^{-1} for Al-Al-OH pyrophyllite vibrations and Al-Al-OH mica vibrations, respectively. The IR spectra in the stretching zone of the three beidellites synthesized at 325°C show that the increase in deficit of charge is associated with an increase in the band surface near 3640 cm^{-1} as compared to the band at 3670 cm^{-1} . Figure 9 shows this trend with two bands at ~ 3620 and ~ 3665 cm^{-1} .

The change in the C/(C+T) ratio of these beidellites with various layer-charge deficits was studied by DTG

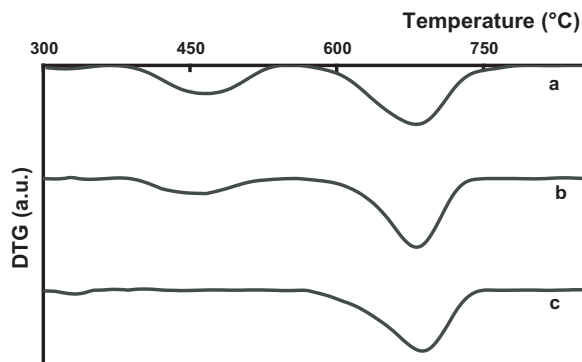


Figure 10. DTG curves of synthetic beidellite samples SB1-325 (a), SB2-325 (b), and SB3-325 (c).

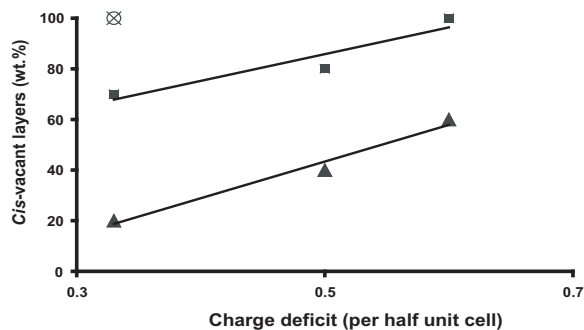


Figure 11. Evolution of the relative proportion of *cis*-vacant layers as a function of the layer charge deficit. ▲: SB_(1,2 or 3)-280 samples; ■: SB_(1,2 or 3)-325 samples; ○: SB1-350; ×: (Klopprogge *et al.*, 1990).

(Figure 10). Sample SB1-325 has a C/(C+T) ratio of 70% and it increases for beidellites with greater layer-charge deficits, with values near 80% and 100% for SB2-325 and SB3-325, respectively (Figure 11).

A second run was synthesized at 280°C and 7.5 MPa (Table 2). Corresponding XRD patterns are presented in Figure 7c,g,j. The C/(C+T) ratio is reported in Figure 11. In the same hydrothermal synthesis conditions, the C/(C+T) ratio increases linearly with the layer-charge deficit.

CONCLUSIONS

Some synthetic beidellites and a natural beidellite were investigated. In the typical hydrothermal conditions of beidellite synthesis as suggested by Klopprogge *et al.* (1990), these samples consist of *cis*-vacant layers, unlike the natural beidellites, which are composed of *trans*-vacant layers. Using lower-pressure and/or temperature conditions, it is possible to synthesize beidellites with a controlled *cis/trans* ratio. A set of beidellites with the same chemical composition and the same layer-charge deficit, but with different *cis/trans* ratio was synthesized at 350°C/25 MPa and 280°C/7.5 MPa. Another set of beidellites with the same *cis/trans* ratio, but with different layer-charge deficits was obtained at 325°C/11.5 MPa and 280°C/7.5 MPa.

These synthetic beidellites are interesting in terms of study of the transformation of smectite to illite or of the study of swelling phenomena.

ACKNOWLEDGMENTS

P. Baillif, O. Rouer, and B. Boukantar (ISTO-Orléans) are thanked for their assistance during this study. J.-M. Douillard is thanked for his valuable comments and suggestions. D.K. McCarty, B. Sakharov, and an anonymous reviewer are thanked for their constructive remarks.

REFERENCES

Besson, G. (1980) Structure des smectites dioctaédriques paramètres conditionnant les fautes d'empilement des

- feuillet. Thèse de l'Université d'Orléans, Orléans, France, 153 pp.
- Besson, G., and Drits, V.A. (1997a) Refined relationships between chemical composition of dioctahedral fine-grained mica minerals and their infrared spectra within the OH stretching region. Part I: identification of the OH stretching bands. *Clays and Clay Minerals*, **45**, 158–169.
- Besson, G. and Drits, V.A. (1997b) Refined relationships between chemical composition of dioctahedral fine-grained micaceous minerals and their infrared spectra within the OH stretching region. Part II: The main factors affecting OH vibrations and quantitative analysis. *Clays and Clay Minerals*, **45**, 170–183.
- Caillere, S., Henin, S., and Rautureau, M. (1982) *Minéralogie des Argiles, 2. Classification et Nomenclature*. Masson, Paris, 182 pp.
- Cases, J.M., Bérend, I., Besson, G., François, M., Uriot, J.P., Thomas, F., and Poirier, J.E. (1992) Mechanism of adsorption and desorption of water vapor by homoionic montmorillonite. 1. The sodium-exchanged form. *Langmuir*, **8**, 2730–2739.
- De Kimpe, C.R. (1976) Formation of phyllosilicates and zeolites from pure silica-alumina gels. *Clays and Clay Minerals*, **24**, 200–207.
- Decarreau, A., Bonnin, D., Badaut-Trauth, D., Couty, R., and Kaiser, P. (1987) Synthesis and crystallogenesi of ferric smectite by evolution of Si-Fe coprecipitates in oxidizing conditions. *Clays and Clay Minerals*, **22**, 207–223.
- Drits, V.A. (2003) Structural and chemical heterogeneity of layer silicates and clay minerals. *Clay Minerals*, **38**, 403–432.
- Drits, V.A. and McCarty, D.K. (2007) The nature of structure-bonded H₂O in illite and leucophyllite from dehydration and dehydroxylation experiments. *Clays and Clay Minerals*, **55**, 45–58.
- Drits, V.A., Besson, G., and Muller, F. (1995) An improved model for structural transformations of heat-treated aluminous dioctahedral 2:1 layer silicates. *Clays and Clay Minerals*, **43**, 718–731.
- Drits, V.A., Lindgreen, H., Salyn, A.L., Ylagan, R., and McCarty, D.K. (1998) Semiquantitative determination of trans-vacant and cis-vacant 2:1 layers in illites and illite-smectites by thermal analysis and X-ray diffraction. *American Mineralogist*, **83**, 1188–1198.
- Eberl, D. (1978) Reaction series for dioctahedral smectites. *Clays and Clay Minerals*, **26**, 327–340.
- Gaboriau, H. (1991) Interstratifiés smectite-kaolinite de l'Eure. Thesis, Université d'Orléans, France, 274 pp.
- Gates, W.P. (2004) Infrared spectroscopy and the chemistry of dioctahedral smectites. Pp. 125–168 in: *The Application of Vibrational Spectroscopy to Clay Minerals and Layered Double Hydroxides* (T. Klopogge editor). CMS Workshop Lectures. Vol 13, The Clay Minerals Society, Aurora, Colorado, USA.
- Granquist, W.T. and Pollack, S.S. (1967) Clay mineral synthesis II. A randomly interstratified aluminum montmorillonoid. *American Mineralogist*, **52**, 212–226.
- Granquist, W.T., Hoffman, G.W., and Boteler, R.C. (1972) Clay mineral synthesis III. Rapid hydrothermal crystallization of an aluminian smectite. *Clays and Clay Minerals*, **20**, 323–329.
- Grauby, O., Petit, S., Decarreau, A., and Baronnet, A. (1993) The beidellite-saponite series: an experimental approach. *European Journal of Mineralogy*, **5**, 623–635.
- Greene-Kelly, R. (1957) The montmorillonite minerals (smectites). P. 140 in: *The Differential Thermal Investigation of Clays* (R.C. Mackenzie, editor). Monograph 2, Mineralogical Society, London.
- Gregg, S.J. and Sing, K.S.W. (1982) *Adsorption, Surface Area and Porosity*. Academic Press, London, 44 pp.
- Hamilton, D.L. and Henderson, C.M.B. (1968) The preparation of silicate compositions by a gelling method. *Mineralogical Magazine*, **36**, 832–838.
- Klopogge, J.T. (2006) Spectroscopic studies of synthetic and natural beidellites: A review. *Applied Clay Science*, **31**, 165–179.
- Klopogge, J.T., Jansen, J.B.H., and Geus, J.W. (1990) Characterization of synthetic Na-beidellite. *Clays and Clay Minerals*, **38**, 409–414.
- Klopogge, J.T., van der Eerden, A.M.J., Jansen, J.B.H., Geus, J.W., and Schuiling, R.D. (1993) Synthesis and paragenesis of Na-beidellite as a function of temperature, water pressure and sodium activity. *Clays and Clay Minerals*, **41**, 423–430.
- Klopogge, J.T., Komarneni, S., and Amonette, J.E. (1999) Synthesis of smectite clay minerals: a critical review. *Clays and Clay Minerals*, **47**, 529–554.
- Lantenois, S. (2003) Réactivité fer métal/smectites en milieu hydraté à 80°C. PhD thesis, Université d'Orléans, Orléans, France, 188 pp.
- Lantenois, S., Champallier, R., Bény, J.-M., and Muller, F. (2007a) Hydrothermal synthesis and characterization of dioctahedral smectites: a montmorillonite series. *Applied Clay Science* (in press).
- Lantenois, S., Bény, J.-M., Muller, F., and Champallier, R. (2007b) Integration of iron in natural and synthetic Al-pyrophyllites: an infrared spectroscopic study. *Clay Minerals*, **42**, 129–143.
- MacEwan, D.M.C. and Brown, G. (1961) *The X-ray Identification and Crystal Structures of Clay Minerals*. Mineralogical Society, London, 143 pp.
- Mackenzie, R.C. (1970) *Differential Thermal Analysis*, Vol. I. Academic Press, London.
- Moore, D.M. and Reynolds, R.C. (1997) *X-ray Diffraction and the Identification and Analysis of Clays Minerals*. Oxford University Press, Oxford and New York, p. 87.
- Muller, F., Drits, V.A., Plançon, A., and Robert, J.-L. (2000) Structural transformation of 2:1 dioctahedral layer silicates during dehydroxylation-rehydroxylation reactions. *Clays and Clay Minerals*, **48**, 572–585.
- Muller, F., Pons, C.-H., and Papin, A. (2002) Study of dehydroxylated-rehydroxylated smectites by SAXS. *Journal de Physique IV*, **12**, 6–17.
- Nakazawa, H., Yamada, H., Yoshioka, K., Adachi, M., and Fujita, T. (1991) Montmorillonite crystallization from glass. *Clay Science*, **8**, 59–68.
- Roux, J. and Volfinger, M. (1996) Mesures précises à l'aide d'un détecteur courbe. *Journal de Physique*, **IV**, 127–134.
- Roy, R. and Sand, L.B. (1956) A note on some properties of synthetic montmorillonites. *American Mineralogist*, **40**, 147–178.
- Suquet, H., Iiyama, J.T., Kodama, H., and Pezerat, H. (1977) Synthesis and swelling properties of saponites with increasing layer charge. *Clays and Clay Minerals*, **25**, 231–242.
- Suquet, H., Prost, R., and Pezerat, H. (1982) Etude par spectroscopie infrarouge et diffraction X des interactions eau-cation-feuillet dans les phases à 14.6, 12.2 et 10.1 Å d'une saponite - Li de synthèse. *Clay Minerals*, **17**, 231–241.
- Torii, K. (1985) Synthesis of trioctahedral smectites. *Journal of the Clay Science Society of Japan*, **25**, 71–78.
- Torii, K. and Iwasaki, T. (1986) Synthesis of new trioctahedral Mg-smectite. *Chemistry Letters* (Tokyo), **12**, 2021–2024.
- Torii, K. and Iwasaki, T. (1987) Synthesis of hectorite. *Clay Science*, **7**, 1–16.
- Torii, K., Asaka, M., and Hotta, M. (1983) Synthesis of silicates. *Japanese Patent* 58/185, 431.
- Trauth, N. and Lucas, J. (1967) Apport des méthodes thermiques dans l'étude des minéraux argileux. *Bulletin du*

- Groupe Français des Argiles*, **XIX-2**, 11–24.
- Tsipursky, S.I. and Drits, V.A. (1984) The distribution of octahedral cations in the 2:1 layers of dioctahedral smectites studied by oblique-texture electron diffraction. *Clay Minerals*, **19**, 177–193.
- Tsipursky, S.I., Kameneva, M.Y., and Drits, V.A. (1985) Structural transformation of Fe³⁺-containing 2:1 dioctahedral phyllosilicates in the course of dehydration. *Proceedings of the 5th Conference of the European Clay Groups* (J. Korta editor). Prague, pp. 569–577.
- Weir, A.H. and Greene-Kelly, R. (1962) Beidellite. *American Mineralogist*, **47**, 137–146.
- Yamada, H., Nakazawa, H., Yoshioka, K., and Fujita, T. (1991) Smectites in the montmorillonite–beidellite series. *Clay Minerals*, **26**, 359–369.
- Yamada, H., Nakazawa, H., Hashizume, H., Shimomura, S., and Watanabe, T. (1994) Hydration behaviour of Na-smectite crystals synthesized at high pressure and high temperature. *Clays and Clay Minerals*, **42**, 77–80.
- Zviagina, B.B., McCarty, D.K., Środoń, J., and Drits, V.A. (2004) Interpretation of infrared spectra of dioctahedral smectites in the region of OH-stretching vibrations. *Clays and Clay Minerals*, **52**, 399–410.

(Received 22 February 2007; revised 17 August 2007; Ms. 1253; A.E. Douglas K. McCarty)